Proceedings of the 10th Asian–Pacific Regional IAU Meeting 2008
August 3 – 6, 2008, Kunming, China
Shuang-Nan Zhang, Yan Li & Qingjuan Yu, eds.

The Southern Binaries Programme of CONZ and CAAM

E. Budding[1,2]
[1] *Carter National Observatory (CONZ), Wellington, New Zealand*
[2] *Astrophysics Research Centre (CAAM), 18 March University of Çanakkale, Çanakkale, Turkey*

Abstract: The 'eclipse method' of stellar astronomy means using the light and colour curves of close binary stars, coupled with spectroscopic information on their radial velocities, to determine absolute parameters, such as masses, radii and luminosities, that are of basic astrophysical significance. Parallaxes can also be deduced and results compared or combined with direct astrometry in some cases. Our programme is aiming such techniques particularly to relatively under-observed, or newly discovered, southern binaries. An end-target is to have clearer information on the relationship of stellar properties to their galactic environment.

A more well-known programme example, allowing us to illustrate procedures and purposes, is the young, Gould's Belt located, multiple system U Oph. Recent high-resolution spectroscopy with the Hercules spectrograph and 1m McLellan telescope of the University of Canterbury at Mt John University Observatory, together with optical and UV photometry are discussed. Information limit optimization techniques (ILOT), with physically realistic fitting functions that include proximity and eclipse effects applied to these data, have been used to find parameters. We also used an ILOT approach for combined eclipse minima timings and HIPPARCOS astrometry to examine the wide orbit of U Oph AB-C. Paczyński's (1970) stellar modelling code has been developed to estimate a likely age, that enables us to relate the system to galactic star formation processes. Such information on this type of young multiple star should assist general understanding of stellar cosmogony.

Key words: ISM: molecules, ISM: structure, instabilities

1 INTRODUCTION

This paper is mainly about (a) high resolution spectroscopy and photometry of southern close (eclipsing) binaries (EBs); (b) analysis with fast and versatile fitting functions taking suitable account of proximity and eclipse effects; and (c) applications to the galactic circumstances of stars.

It is fairly well-known that, as well as stellar absolute luminosities, masses, radii (R) and temperatures, distances (parallaxes Π) can be derived from data on normal EBs (Budding et al. 2005a). Knowing the visual magnitude m_V, the method involves a relation such as

$$\log \Pi = 7.450 - \log R - 0.2 m_V - 2F'_V \qquad (1)$$

where the 'flux' F'_V is given in terms of the effective temperature T_e and bolometric correction BC as $F'_V = \log T_e + 0.1BC$, but also separately by an empirical dependence on the colour (e.g. $B-V$) that may hold very well for a particular group of stars (e.g. Population I Main Sequence stars).

Semeniuk (2000) pointed out that parallaxes obtained by this method (H.N. Russell's (1948) *Royal Road*) could have an accuracy surpassing that of HIPPARCOS (ESA, 1997) if care was taken about the choice of binaries and adopted flux-colour relation. Only one star in ∼1000 is an EB, but the fact that eclipses can be observed as far as stars can be individually monitored gives the method wide significance (cf. Figure 1).

Moreover, careful monitoring of EBs not uncommonly reveals the presence of companion ('third body') objects, found from photometry, spectroscopy, or irregularities in recorded times of minimum light ('O–C curves'). In such cases, HIPPARCOS astrometry can sometimes be usefully reanalysed, to check the geometry of the wide orbit. The outcomes from such analysis include component masses for multiple systems.

Recent trends of application for the eclipse method have been to greater distances within our own Galaxy (Paczyński, 1996) and outward to the nearest neighbouring galaxies (the LMC & SMC: Guinan et al. 1998) and beyond. Nowadays, analysable light curves are available for EBs within the Local Group of galaxies. Spectrometry has been applied to candidate objects in the nearer galaxies using ground-based large telescopes (Ribas et al. 2002). Improved filter systems with greater analytical power are also being introduced. The use of selected filter systems has been significant in probing star formation regions and assessing population types (e.g. Dickow et al. 1970).

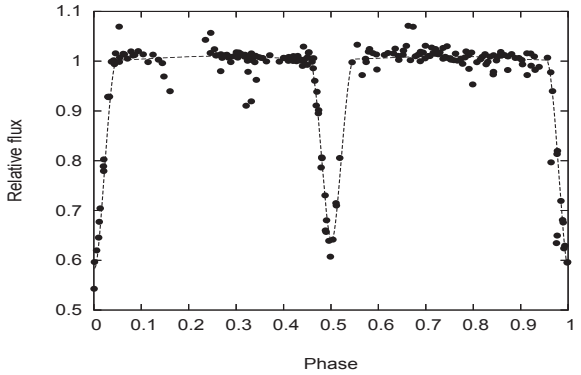

Figure 1. Preliminary extracted MOA-project light curve of the newly discovered ∼18th mag ecliping binary GB7-5-69. The derived period (after elimination of a few very stray points) of 3.326812 days, when combined with the fractional radii derived from the curve-fitting, yields a Main Sequence (MS) like pair of stars – say B8-B9 types – with a total mass of around 6 solar masses. The component radii then turn out about 2.5 times that of the Sun, which is consistent with an early MS condition. The main parameters of the fitting are: fractional luminosities L1 & L2: 0.59 and 0.41; fractional radii: 0.149 & 0.147; orbital inclination 85.6 deg. For more details on the MOA programme, refer to the article of P. Yock in this volume.

Radial velocity (rv) measurements form a relatively underdeveloped subject for binaries south of declination about $-20°$. Apart from stars listed by Rucinski (1999), candidates also came from the papers of Demircan (2000) and Nitschelm (2004), and include: V822 Aql, QS Aql, R Ara, V486 Car, ν Cen, V716 Cen, V831 Cen, V883 Cen, V964 Cen, AT Cir, HZ CMa, α^3 Cru, λ Cru, W Cru, CH Cru, PP Hya, β Hyi, BG Ind, BR Ind, λ Lib, γ Lup, σ Lup, GG Lup, KT Lup, V727 Mon, η Mus, FH Mus, KR Mus, 7 Oph, U Oph, δ Ori, ψ Ori, V1371 Ori, TV Pic, AE Pic, V410 Pup, δ Sco, μ_1 Sco, V718 Sco, V1003 Sco, μ Sgr, υ Sgr, RS Sgr, PT Vel, HR 6003, NSV 20610. Beside these mainly hot young stars, some candidate binaries were selected from among cooler active and contact objects, observed mainly in 2007, but the emphasis in the present article is on hot stars.

2 PROCEDURES WITH CLOSE BINARIES

The application of EBs to direct checking of basic stellar parameters was the subject of a number of seminal publications of D.M. Popper (e.g. Popper, 1998). We seek to follow such work with further detailed studies. One important concept is the limit to the information content of given data-sets. This point gave rise to the *information limit optimization technique* (ILOT), wherein modelling tries to parametrize to this limit, neither producing excessive detail, nor underrepresenting through over-simplification.

Another point is to check underlying physical assumptions, such as in flux-colour relationships. There would be, in general, some dependence on the galactic situation in adopted formulae. An approach to studying galactic environment thence arises, via testing flux-colour formulae or examining spectrophotometric effects in selected EBs. In what follows we shall concentrate on the programme star U Oph, for which there are anomalous absorption effects in the line

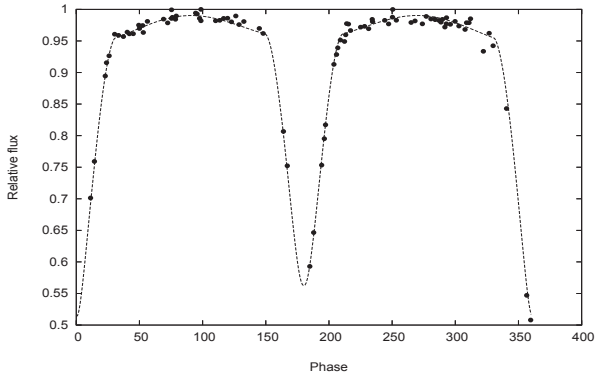

Figure 2. Fitting to HIPPARCOS 'V' light curve of U Oph.

of sight. These suggest a relationship with some relatively recent star-formation region in the Disk.

Fast and robust curve-fitting programs that take into account realistic and detailed approximations for proximity effects in close binary stars have been developed and applied. These give the photometric flux l_c at orbital phase ϕ (cf. Budding and Demircan, 2007, for notational details):

$$l_c(\phi) = U - L_1\alpha(r_1, r_2, i, u_1; \phi) + \Delta L \ , \tag{2}$$

where the photometric perturbation

$$\begin{aligned} \Delta L \quad = \quad & \{\Delta L - \Delta_\alpha L\}_{\rm ell}(\tau_i, q_i; a_j)L_1 + \\ & + \{\Delta L - \Delta_\alpha L\}_{\rm ref}(E_i, q_i; a_j)L_1 \ , \end{aligned} \tag{3}$$

has $i = 1, 2$ for the two stars; and $j = 1, n$ for n stellar parameters in the model.

These formulae specify proximity effects arising from 'ellipticity' (tidal and rotational distortions of figure) and 'reflection' (mutual irradiation) as additive terms. The standard treatment proceeds to the fifth order in the relative radii $r_{1,2}$. The fitting functions adopt regular spherical harmonic expansions, as developed through the classical papers of Clairaut, Laplace, Tisserand, Poincaré, Chandrasekhar and others, and summarized in Kopal's (1959) monograph. Although the effect of tides on tides is neglected in this approximation to the solution of the relevant Poisson equation (as in the 'Roche models' of other codes), it does allow a finite internal density distribution to be included. Results of an application of such fitting to photometry of U Oph are shown Figures 2 and 3.

While such modelling is fairly commonplace for the photometric variation, the existence of an essentially parallel treatment for radial velocities is less well-known, although it was also spelled out by Kopal (1945). This is perhaps because the scale of proximity effects in comparison to the basic Keplerian velocity term is quite small, and until relatively recently would have been typically below errors of measurement. The relevant expression is:

$$v_c(\phi) = v_0(\phi) + v_{\rm rot}\alpha^1(r_1, r_2, i, u_1; \phi) + \Delta v \ , \tag{4}$$

where the rv perturbation Δv is given by:

$$\begin{aligned} \Delta v \quad = \quad & \{\Delta v - \Delta_{\alpha^1} v\}_{\rm ell}(\tau_i, q_i; a_j)v_1 + \\ & + \{\Delta v - \Delta_{\alpha^1} v\}_{\rm ref}(E_i, q_i; a_j)v_1 \ . \end{aligned} \tag{5}$$

$v_0(\phi)$ contains the regular Keplerian velocity with the velocity of the centre of mass added: $v_0(\phi) = K_1(\cos(\omega + \nu) +$

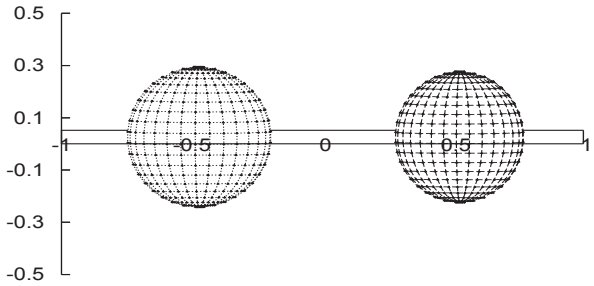

Figure 3. GNUPLOT rendering of U Oph model at elongation showing distortions of figure corresponding to MS-like mass distribution.

$e\cos\omega)+\gamma$. The term $v_{\rm rot}\alpha^1(r_1, r_2, i, u_1; \phi)$ gives the eclipse (Rossiter) effect. This depends on the α^1 integral, which is formally similar to the normal eclipse α-integral (Kopal, 1942). Δv accounts for proximity effects, following a similar form to ΔL in (3). The component $\Delta_{\alpha^1} v$ yields the proximity effect in eclipse: it is zero outside of eclipse phases.

Binary star rvs have been measured using correlation techniques for a few decades. This approach has tended to replace earlier methods based on direct measurements of Doppler shifted lines, but there are still problems for EBs, particularly away from elongation phases. Rucinski (2005) noted the importance of a better awareness of line profile properties for accurate rv determination (see also Lu & Rucinski, 1999). Our group is experimenting with fitting function forms for stellar spectral lines (Budding et al. 2005b). Aside from proximity effects, profiles would also show signs of the environment, in consequence of evolution, age or composition effects. Rucinski (2005) pointed out that profile-based analysis shows up a surprisingly high incidence of third components to very close, or contact, binaries: a point having cosmogonic significance.

Rucinski has given attention to new EBs identified by the HIPPARCOS survey for which there is little prior information. While the David Dunlap Observatory survey of northern systems within their magnitude reach is by now almost complete, there remains a distinct gap for the Southern Hemisphere. The Mt John Uninversity Observatory (MJUO) in New Zealand is at a comparable southerly latitude to the northerly one of Toronto, and available telescopes are of comparable size. MJUO has important access to the Centre of Galaxy region, while any study that takes into account galactic binary occurrence should have complete sampling with respect to galactic longitude. Such points influenced the choice of observing location for this programme.

2.1 Specific points about observations

MJUO's 1-metre McLellan Telescope with focal ratio f/13.5 has been used for the spectroscopic observations. The 0.6 m Optical Craftsmen has provided supplementary photometric data. Spectrograms were mostly obtained with the HERCULES échelle spectrograph with resolution ∼70000 operating in near-vacuum conditions. Images were secured using a Fairchild 486 CCD 4k × 4k back-illuminated chip in an SI 600 series cryogenically cooled camera with pixel size 15 μ (cf. Hearnshaw, 2002 for further details). The camera arrangement used for U Oph recorded between ∼7090 Å (order 80) and ∼4500 Å (order 126). Preliminary data reduction was performed on-site using the Hercules Reduction Software Package (HRSP) (Skuljan and Wright, 2007). MJUO's AAVSO CCD camera with BVRI (Cousins) filters has been used for photometry. Further filter-sets are under consideration. Observations hitherto have been carried out over about 50 nights in Apr-May and Aug-Sep in 2006 and about 20 nights in Sep-Oct 2007.

Figure 4 gives three examples of the He I ∼5875.64 Å lines near elongation in the programme stars η Mus, U Oph and V831 Cen, showing the progressive effects of increasing proximity. The problem noted by Rucinski (2005) becomes evident, particularly with the the shallow, highly broadened lines of V831 Cen. The He I line profiles of the components of U Oph, for example, spread over 5 Å each; i.e. over 250 km s^{-1} in velocity. Precision in fixing the line centroid should be thus be better than 0.5% of this width if rvs are to be specified to ∼1 km s^{-1}. There are typically 5 pairs of He I lines in the available range of the spectrograph, together with a half dozen much weaker features. Some Balmer lines are available, but their large intrinsic broadening exaggurates the blending problem, even at elongation, while there might be additional complications due to component interactions. Generally, rvs of the hot EBs in this programme depend on movements of the He I lines.

Figure 4 also shows the 97th order of the star ν Cap (= HD193432). This appears in R.E. Wilson's (1953) catalogue with an rv of 2 km s^{-1} and forms a possible comparison object for cross correlation. If can be seen that sufficiently well separated line pairs, as with η Mus, would allow separation of corresponding peaks in the cross correlation function (ccf), either with one selected (elongation) spectrum of the variable or ν Cap. However, for closer pairs at most intermediate phases the blending of individual lines simply transposes into merged peaks in the ccf. The components' inherent line profiles have to be understood if their velocity separation is to be properly recovered.

2.2 Fitting binary radial velocities

The importance of rv data to unambiguous interpretation of EBs was noted in, for example, Marino et al.'s (2007) discussion of RW Dor, where completely different physical models (MS-like or post mass-exchange) can fit a given light curve to the same accuracy. Figure 5 shows some preliminary data reduction for the spectrograms of U Oph (NB the rvs shown are not corrected for the vacuum to air displacement of ∼ 84 km s^{-1}). Systematic displacements from the primary's expected simple Keplerian sinusoid (the model curve in the out-of-eclipse phases) are evident; in the sense that the elongations appear slightly flattened and conjunction region steepened. Similar effects were noticed in the rvs of Holmgren et al. (1991). Since these trends qualitatively resemble proximity effects, it was tempting to search for

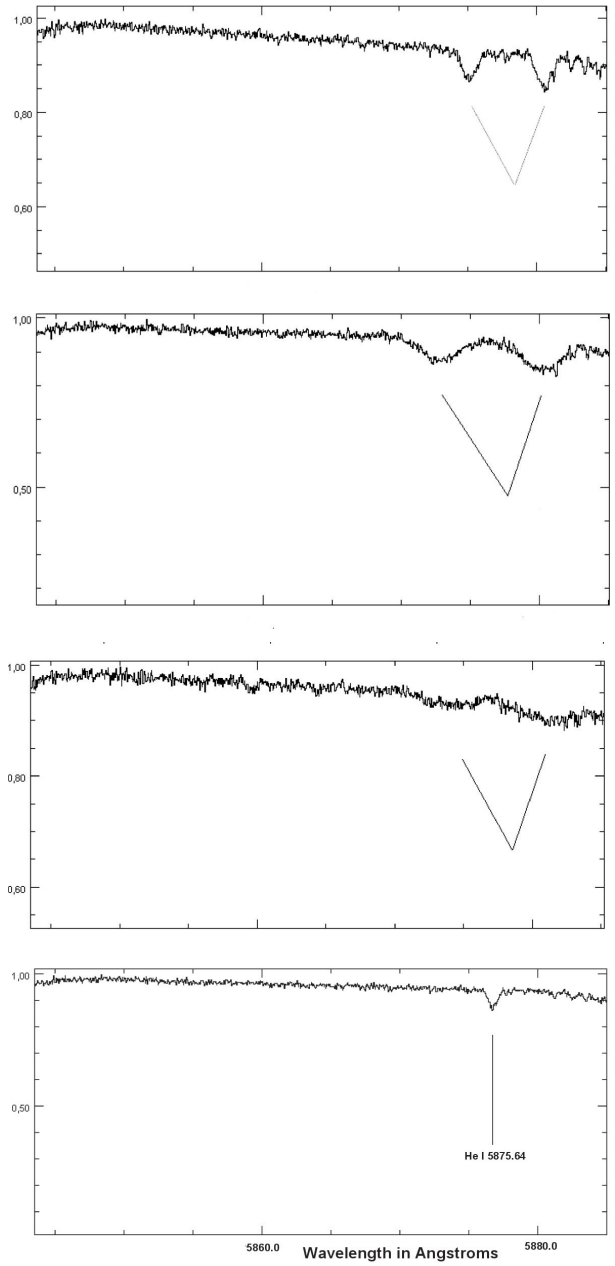

Figure 4. Spectral order number 97 showing region of He I 5876 lines (top down) η Mus, U Oph, (c) V831 Cen and ν Cap.

corresponding parameters in applying the fitting function of Equ (4) in an ILOT program. As well, the eclipse phases suggest a Rossiter effect. While this has been exaggurated in the model shown, the procedure allows for independent evaluation of the rotation velocity from the Rossiter effect.

It turns out, however, that irregularities like those visible in Fig 5, which can be seen to be on the order of tens of km s^{-1} are much too large to be due to proximity effects of the kind discussed by Kopal (1959). Those are on the order of 1 km s^{-1} or less: certainly the ellipticity distortions are too small to explain these differences, and would be barely measurable in the rv determinations presently considered. The Sterne-Kopal theory of the 'reflection effect' only models line centre shifts due to illumination, however. Mutual

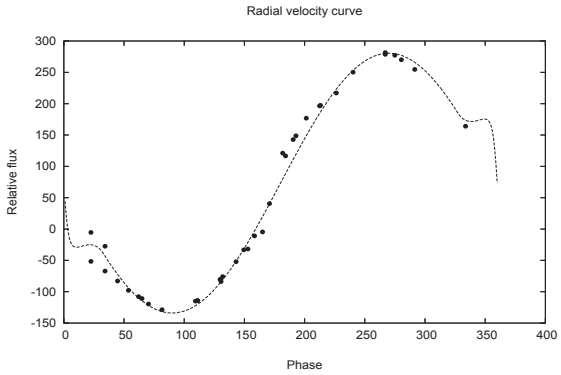

Figure 5. Preliminary rv curve of U Oph A with a demonstration of rv modelling.

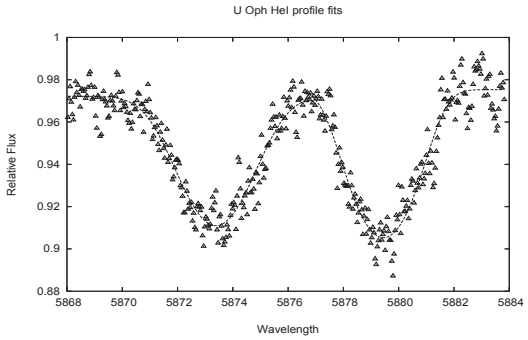

Figure 6. He I 5876 lines at elongation modelled by the dish-gaussian convolution of Eqn 7.

heating may well result in longitudinal photospheric motions that could enhance observed anomalies, but a full exposition of this awaits implentation (cf. Kopal, 1988). Meanwhile, it should be noted that systematic effects may occur in measured rvs that are greater in scale than standard modelling of binary distortions. Fitting of the rv curve is, however, a later step. Before that, we should examine how profile properties relate to the Doppler shifts.

Lines of low optical depth, like the HeI lines here, can be modelled from the well-known dish-shaped form of Shajn & Struve (1929), giving the line depth I_d in dependence on a projected rotational velocity scaled wavelength $x = (\lambda - \lambda_m)c/\lambda_m v_{\rm rot} \sin i$, λ_m being the line's mean wavelength, i the incination and c the velocity of light, as:

$$I_d(x) = I_0 - 3I_c\{(1-u)\sqrt{(1-x^2)} + \pi u(1-x^2)/4\} \ , \quad (6)$$

for $-1 < x < 1$, with $I_d(x) = I_0$ for $x < -1, x > 1$ (u is the coefficient of limb-darkening). But, for a more realistic representation, this form can be convolved with a broadening term arising from thermal or turbulence effects, taken to be gaussian, $I_g(x) = \exp(-x^2/2\sigma^2)$. At x_1, we then have

$$I(x_1) = \int I_d(x).\exp\{-(x-x_1)^2/2\sigma^2\}\}{\rm d}x \ . \quad (7)$$

Given i and u, we can optimize the profile fitting for the parameters $v_{\rm rot}$, σ, λ_m, I_0 and I_c. Figure 6 shows such a fitting applied to a pair of He I (5876) profiles, yielding, for the primary: $I_0 = 0.975 \pm 0.005$, $I_c = 0.059 \pm 0.007$, $\lambda_m = 5879.451 \pm 0.026$, $v_{\rm rot} \sin i = 104.7 \pm 1.6$ km s^{-1}, $\sigma = 12.9 \pm 0.8$; and for the secondary: $I_0 = 0.972 \pm 0.005$, $I_c =$

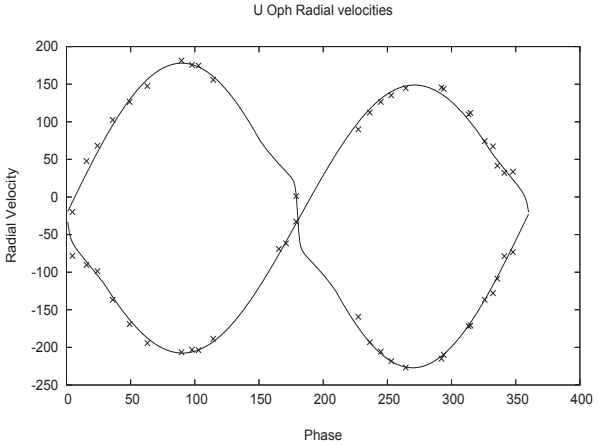

Figure 7. ILOT fitting to adopted measures of U Oph rvs.

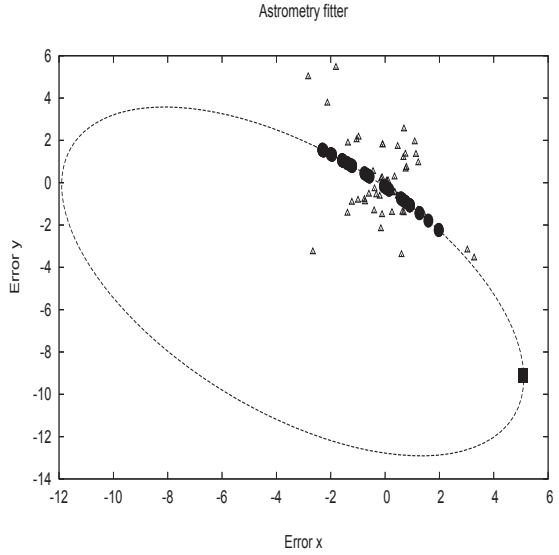

Figure 8. The wide orbit of U Oph AB-C. The HIPPARCOS positions are marked by triangles, while the full circles show the model's orbit positions for corresponding times. The 1981.36 periastron position is indicated by a full square.

0.052 ±0.008, λ_m = 5873.390 ±0.029, $v_{\rm rot}$ sin i = 97.7 ±1.5 km s^{-1} and σ = 23.2 ±1.0. While ILOT optimization aims at minimal model adequacy, Fig 6 suggests the inclusion of proximity effects in future developments to profile fitting.

The finally adopted U Oph rv data-set and its fitting are shown in Figure 7, and the corresponding main absolute parameters are: $K_{1,2}$ = 180.0 ±1.3, 202.7 ±1.2 km s^{-1}; V_γ = –15.8 ±1.4 km s^{-1}; $M_{1,2}$ = 5.13 ±0.08, 4.56 ±0.07 M$_\odot$; $R_{1,2}$ = 3.41 ±0.03, 3.08 ±0.03 R$_\odot$; with $T_{e,1}$ set at 17200 K and $T_{e,2}$ at 16200 K. More details on this system have been given by Budding et al. (2008).

3 MULTIPLE STELLAR SYSTEMS

For systems within a few 100 pc, the analysis of HIPPARCOS astrometric data has been a productive means of further study of the increasing number of EBs found with companion stars (e.g. Bakış et al. 2006). This gains significance when there is also good coverage of times of eclipse minima. In the case of U Oph, Wolf et al.'s (2002) O – C curve-fitting forms a useful source of parameters that can be combined with the astrometric data. The inclination of the wide orbit becomes derivable, allowing subsequent evaluation of the mass of the third star. The nodal angle Ω, referring the orientation of the wide orbit to the equatorial coordinate system, can also be found. The position of the bright EB at any particular time involves the time of periastron passage T_0, which, according to Wolf et al. (2002), was at 1981.36, some 7.4 y before the HIPPARCOS initial epoch.

Figure 8 shows the result of ILOT fitting of a Keplerian astrometric orbit to the postions of U Oph (AB) as measured by HIPPARCOS. The corresponding derived parameters are: P = 38.0 ±0.2 y; i = 57°±3°; Ω = 46°±4°. Other orbital parameters were taken from Wolf et al. (2002). A slightly greater period than that of Wolf et al. was found to give a better fit (cf. also Vaz et al. 2007). Besides these, the fitting determines the shifts $\Delta\alpha \cos\delta$ = –1.7 ±0.3 mas and $\Delta\delta$ = –5.0 ±0.2 mas, that locate the AB-C centre of mass with respect to the centroid of the HIPPARCOS measures (i.e. the origin). The HIPPARCOS catalogue specifies such measures as 'errors' from the centroid (on the assumption of no orbital motion). The (reduced) chi-squared variate χ^2/ν = 1.7 for this fitting is calculated for an adopted individual HIPPARCOS positional error of 2 mas.

Applying Kepler's law to the derived orbit we find the mass of U Oph C as 0.83 $M_\odot$, which is supported by separate photometric evidence. U Oph C is a somewhat more massive star than U Oph D – the 12th mag visual companion of the system. This quadruple configuration of U Oph is then reminiscent of Ambartsumian's (1949) scenario of the heirarchical relaxation of young multiple stars.

4 EVOLUTION AND GALACTIC CONTEXT

Theoretical isochrones for Gould's Belt member stars in selected regions of the Sco-Cen OB2 Association were given by Bertelli (2002). From locating U Oph on such isochrones, noting also its position in the sky, it is found that (a) the system could be a member of Gould's Belt, but (b) its stars are at least as old as most stars of Sco-Cen OB2, which started to form 20-30 My ago. U Oph may be older than that, but we argue for an age closer to the ∼30My of Kämper (1986) than the 63 My of Holmgren et al. (1991). The latter age corresponds to what is thought to be the initial time of formation of Gould's Belt. The proper motions of U Oph indicate that it has moved to increasing longitude away from the direction of Sco-Cen OB2 (de Zeeuw et al. 1999), but dynamical interactions complicate such interpretations for multiple stars.

Beside H-R diagram tests of evolutionary models, Vaz et al. (2007) looked to mass and radius parameters, as against colour-dependent ones. We have followed similar ideas. There are, in fact, various possible approaches to such testing: for example, the values of apsidal motion constants can be used for eccentric systems having relevant data. However, taking into account the full range of factors determining observable properties of stars engenders caution. Thus, the metal content would be an interesting parameter to relate to galactic environment if it could be reliably deter-

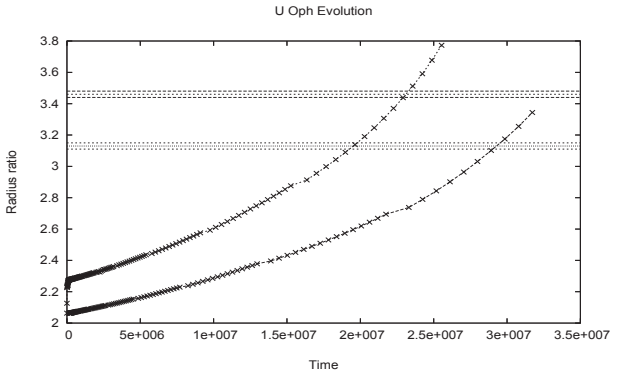

Figure 9. Evolution of the two radii of the components of U Oph according to the Paczyński (1970) code. The observed radii (with their error bounds) are shown as horizontal lines.

mined. But if we allow metallicity to vary in evolution calculations, we should keep in mind that the run of opacities from different authors can produce comparable changes of net stellar observables, even for the same metallicity; while theory, as well as practice, for such calculations continues to be developed (İnlek et al. 2008).

We have used the public-domain stellar modelling codes of Paczyński (1970) to examine the structure and evolutionary status of U Oph. Some results are shown in Figure 9. The measured radius of the primary component, in this diagram, is attained at about 23 My, with 29 My for the secondary; i.e. an average age of ∼25My can be inferred. The significant differences between the two ages seem irreconcilable with the errors of the radii, however. Although it would be expected that the ages and initial compositions should be the same for both stars (Andersen, 1993), tests of the Paczyński code in the vicinity of the adopted masses show high sensitivity of the ZAMS radius to assigned initial conditions. Figure 9 has been constructed using the rather high metallicity Z = 0.03 that could feasibly apply to young Disk stars. Such a metallicity produces a relatively large initial radius, however, so the time taken to reach the observed radius becomes shorter. The lower, more typical, metallicity Z = 0.02, considered by Vaz et al. (2007), takes our average age up to around 38 My, close to the 40My of Vaz et al. Whether the age discrepancy for the two components could be explained by small individual composition difference, or something else not considered in the simple modelling experiments performed so far, remains to be found out. In view of the various uncertainties, we believe a realistic age estimate for the U Oph system can be put as 30-40 My.

ACKNOWLEDGMENT

I am grateful to the LOC and SOC of this Meeting for their invitation and generous support. Support was also given by the Physics Department of the 18th March University of Canakkale, Turkey and the Royal Astronomical Society of New Zealand. Helpful comments on this work were made by Profs. O. Demircan and A. Erdem, and also Prof. J. Hearnshaw. V. and H. Bakış, D. Doğru and B. Özkardeş also gave appreciated assistance with praticalities, as well as Dr. D. Wright and staff at the Mt John University Observatory. The programme has received official support from TUBITAK (Turkish Science Research Council) and the Carter Observatory of New Zealand.

REFERENCES

Ambartsumtan, V.A., 1949, AZh 26, 8.
Andersen, J., 1993, ASP Conf. Ser. 40, 347.
Bakış, V., Budding, E., Erdem, A., Bakış, H., Demircan, O., Hadrava, P., 2006, MNRAS 370, 1935.
Bertelli, G., 2002, EAS Publ. Ser. 2, 265.
Budding, E., Sullivan, D., Rhodes, M., 2005, IAU Coll 196, 386.
Budding, E., Bakış, V., Erdem, A., Demircan, O., Iliev, L., Iliev, I., Slee O.B., 2005, Ap&SS 296, 371.
Budding, E. & Demircan, O., 2007, *An Introduction to Astronomical Photometry*, Cambridge Univ. Press.
Budding, E., İnlek, G., Demircan, O., 2008, MNRAS (preprint).
de Zeeuw, P.T., Hoogerwerf, R., de Bruijne, J.H.J., 1999, AJ 117, 354
Demircan, O., 2000, NATO Sci. Ser. C, Math. Phys. Sci. 544, 623.
Dickow, P., Gyldenkerne, K., Hansen, L., Jacobsen, P.-L., Johanson, K.T., Kjaergaard, P., Olsen, E.H., 1970, A&AS 2, 1.
ESA, 1997, *The HIPPARCOS and Tycho Catalogues*, ESA SP-1200
Guinan, E.F., Fitzpatrick, E.L., Dewarf, L.E., Maloney, F.P., Maurone, P.A., Ribas, I., Pritchard, J.D., Bradstreet, D.H., Giménez, A., 1998, ApJ 509, 21.
Hearnshaw, J.B., Barnes, S.I., Kershaw, G.M., Frost, N., Graham, G., Ritchie, R., Nankivell, G.R., 2002, Exp. A 13, 59.
Holmgren, D.E., Hill, G., Fisher, W., A&A 248, 149.
İnlek, G., Böke, A., Yılmaz, O., Budding, E., 2008, Turk J. Phys. 32, 65.
Kämper, B.C., 1986, Ap&SS 120, 16.
Kopal, Z., 1942, Proc. Amer. Phil. Soc. 85, 399.
Kopal, Z., 1945, Proc. Amer. Phil. Soc. 89, 517.
Kopal, Z., 1959, *Close Binary Systems*, Chapman & Hall, London & New York.
Kopal, Z., 1988, Ap&SS 144, 557.
Lu, W. & Rucinski, S. 1999, AJ 118, 515.
Marino, B.F., Walker, W.S.G., Bembrick, C., Budding, E., 2007, PASA 24, 199.
Nitschelm, 2004, ASPC 318, 291.
Paczyński, B., 1970, AcA 2, 20.
Paczyński, B., 1996, IAU Symp. 173, 199.
Popper, D., 1998, PASP 110, 919.
Ribas, I., Fitzpatrick, E.L., Maloney, F.P., Guinan, E.F., Udalski, A., 2002, ApJ 574, 771.
Rucinski, S. 1999, JRASC 93, 186.
Rucinski, S. 2005, HiA 13, 458.
Russell, H.N., 1948, *Harvard Obs. Mon.* No. 7, p 181.
Semeniuk, I., 2000, AcA 50, 381.
Shajn, G., Struve, O., MNRAS 89, 222.
Skuljan, J., Wright, D., 2007, *Hercules Reduction Software Package (HRSP)*, vers. 3, Univ. Canterbury, New Zealand.
Vaz, L.P.R., Andersen, J., Claret, A., 2007, A&A 469, 285.
Wilson, R.E., 1953, *General Catalogue of Radial Velocities*, Carnegie Inst., Washington.
Wolf, M., Harmanec, P., Diethelm, R., Hornoch, K., Eenens, P., 2002, A&A 383, 533.